Surface Science 733 (2023) 122307

Contents lists available at ScienceDirect

Surface Science

journal homepage: www.elsevier.com/locate/susc

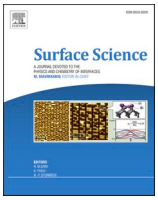

Ag-oxide signature in Ag 3d photoelectron spectra: A study on free nanoparticles

E. Tzomos [a], M.-H. Mikkelä [b], G. Öhrwall [b], O. Björneholm [c], M. Tchaplyguine [b,*]

[a] Department of Physics, Synchrotron Radiation Research Division, Lund University, Box 118, Lund 22100, Sweden
[b] MAX IV Laboratory, Lund University, Box 118, Lund 22100, Sweden
[c] Department of Physics and Astronomy, Uppsala University, Box 516, Uppsala 75120, Sweden

A B S T R A C T

Over decades the Ag 3d-level binding energy has been puzzling researchers with its unusual sign and value in silver oxides. For the absolute majority of metals, the metal-to-oxide binding energy shifts are positive and depend significantly on the oxidation state, while in Ag-oxides the oxide shift was time after time reported negative, small, and close for the two very different Ag(I) and Ag(III) oxidation states. In the current work, a photoelectron spectroscopy (PES) investigation on the *in-situ* created free nanoparticles simultaneously containing both metallic silver and silver-oxide parts provided the grounds to reconsider the old consensus on the Ag-oxide shifts. The Ag 3d energies for the metallic and the oxide parts established in the current experimental work allowed estimating a ≈ 1.2 eV *positive* shift for the realized oxidation state. This estimate was made possible by using a *beam* of *free* nanoparticles with finely controlled composition. The PES experiments on such a beam allowed for a continuous and fast renewal of the poorly conducting sample and for a reliable and accurate calibration relative to vacuum. The constant oxide shift observed at several different oxidation conditions, as well as the relatively narrow and symmetric oxide peaks, point to one dominating oxidation state being present in the particles.

1. Introduction

The spectroscopic signature of silver oxide -as seen by photoelectron spectroscopy (PES)- has been a matter of keen interest for half a century, ever since the pioneering work of Schön [1]. The oxide Ag 3d core-level binding energy fell early under scrutiny [2–4] motivated by catalysis [5], but with time the interest also developed a fundamental character: While for most metals the core-level binding energies were as a rule *higher* in the oxides than in the corresponding metallic samples [6–10], the silver-oxide Ag 3d response was time after time detected at *lower* binding energies [1–12]. In other words, the characteristic metal-to-oxide energy difference, the oxide shift, was negative. Moreover, for the two very different Ag(I) and Ag(III) oxidation states the oxide shifts were as a rule reported to be close: For the Ag(I)-oxide – ≤0.4 eV[1-3,11,13], and for the Ag(III)-oxide, in which the Ag 4d-shell is open, – ≤0.8 eV [1,4,14]. Noteworthy, in case of co-presence of both oxides in a sample, such shifts could not be resolved in most of the cited works since the total instrumental broadening due to the light source (Al K_α with $h\nu \approx 1487$ eV or Mg K_α with $h\nu \approx 1254$ eV) and electron-energy analyser was ≤1 eV [1–4,6,11,12]. However, even if the instrumental broadening were narrower, the Ag 3d *natural* width of ≈0.3 eV [15] would make it practically impossible to resolve Ag(0) and Ag(I), or Ag(I) and Ag(III) pairs of states with such close binding energies. The negative, unusually small, and close oxide shifts contradicted the expectations — to a degree that researchers attempted measuring the oxide Ag 3d spectra again and again, trying various approaches to overcome the inherent difficulties in such experiments. One of the crucial obstacles was the uncertain sample composition and its insufficient purity [8]. In the earlier experiments, which laid the grounds for the wide acceptation of the negative and small oxide-shifts, the commercial oxide powder was usually pressed into a pellet, and the oxide, though known to be thermally unstable, was subsequently heated before the measurements —to reduce the contaminants' amount. While it was clear that such treatment could change the composition [2–4], little could be done to improve the situation- if starting from the commercial powders. With the time, researchers managed to produce Ag oxides *in-situ*, from a metallic precursor, using various methods, with the oxygen-plasma treatment being one of the most "clean" and efficient methods [2,8,13]. However, while the progress was reached in the sample fabrication, another obstacle – coming from the side of the binding energy calibration – occurred to be more difficult to overcome. In surface science, a standard reference point for the core-level binding-energy is the Fermi-energy (FE) level of the substance or of the electron analyser. For a metallic sample, its FE-level, which also defines its work-function (WF), can be detected

* Corresponding author.
E-mail address: maxim.tchaplyguine@maxiv.lu.se (M. Tchaplyguine).

https://doi.org/10.1016/j.susc.2023.122307
Received 12 January 2023; Received in revised form 14 April 2023; Accepted 16 April 2023
Available online 17 April 2023

using PES —as an onset of the metallic valence band. This should, in principle, allow for an accurate binding energy calibration – relative to the Fermi level. However, for silver there was a problem also here: the *metallic* valence Ag 5s-band could not be detected at hν >1000 eV [3,4,11,12] —due to the low ionization cross-section at such high photon energies [16]. For the oxides, which are semiconductors or isolators, the FE-level lies in the gap, and is thus not accessible by PES. In this case, the valence-band onset defines the HOMO (Highest Occupied Molecular Orbital) energy. For the oxide-spectrum calibration, the alignment of the Fermi levels of the sample and of the analyser is usually assumed [17]. This alignment, however, can break down when the poorly conducting oxide sample accumulates a positive charge under the ionizing irradiation. In the analysis of the early PES results on Ag-oxide powder-samples, some "correlation" of the HOMO edge relative to the reference FE-level had to be done (e.g. [3,4]) – to compensate for the sample charging which was not controlled. Also in another early work [2], where the Ag foil was plasma-oxidized *in-situ*, as well as in the relatively recent studies [11,12], the charging was not controlled, while the authors discussed its possible influence. Anyway, even if standard measures are taken to compensate for charging – by irradiating the sample with a flow of electrons from an electron flood gun, the calibration may differ from one oxide to another –and this within the same experiment. This was the case, for example, in the study on two *tin-oxides* [18,19], for which the oxide shifts were also a matter of debate for decades and for which commercial oxide powders were also often used. In works [18,19], where the flood gun was implemented, the adventitious carbon peak −used for calibration− differed by ≈1 eV in the SnO and SnO_2 Sn 3d spectra. Flood-gun us giving the calibration uncertainty of 1 eV would not be worth an effort for Ag-oxides in the works discussed above, since the Ag 3d spectra were recorded with the instrumental broadening of ≤1 eV. Moreover, at such experimental conditions, the presumably small difference in the FE between the metal and the oxide – also about 1 eV [2] – complicated the calibration.

Early synchrotron facilities made a wider range of photon energies available for PES, however even then the Ag 3d spectra and the valence spectra often could not be recorded at one and the same photon energy, and thus could not be unambiguously referenced to each other. For example, in the widely cited work [2], the valence spectra were recorded with a low hν and high resolution at HASY Lab, while the Ag 3d level was still studied with Al K_α. And, as noted above, necessary for the calibration FE "edge" of *metallic* silver could not be detected at hν≈1487 eV.

Eventually, modern synchrotrons finally provided access to photon energies favourable for recording the Ag 3d spectra at high resolution [9,10,13]. The work [9,10] on a *surface-oxide single monolayer* is the one where PES resolved two types of Ag atoms differently coordinated to oxygen, with the more abundant type appearing 0.6 eV *below* the metallic signal. The distinction of the two close Ag 3d peaks marked a qualitative achievement, however, it left the puzzle of the "bulk" Ag-oxide unsolved.

As mentioned above, this "puzzle" may have been created by how the oxide Fermi level and, correspondingly, the Ag 3d response were calibrated. Recently, new opportunities appeared for the experimental determination of the valence and core-level energies: it became possible to study *free unsupported* metal and metal-oxide nanoparticles in a beam by synchrotron-based PES [20]. A study on a beam provides access to the *absolute* binding energy calibration –relative to the vacuum and not to the substrate/spectrometer Fermi level. This makes it possible to overcome the uncertainty with the FE-level alignment and calibration discussed above. Moreover, a study on a beam of particles eliminates the problem of charge accumulation on the sample since the sample is continuously and quickly renewed in the ionization volume. In the current work, studying *free nano*particles containing both Ag-metal and Ag-oxide by PES, we were able to determine the Ag 3d oxide binding energy and the oxide shift directly from one and the same spectrum referenced to vacuum. In contrast to the accepted picture, the oxide Ag 3d energy was detected to be *higher* than in metallic silver – by more than 1 eV.

2. Experiment

2.1. Sample production and experiment geometry

Free nanoparticles containing Ag-oxide were created using an in-house built nanoparticle source. The primary atomic-Ag vapour was produced by a DC-magnetron-sputtering gun placed inside a cryostat cooled by a continuous flow of liquid nitrogen. A sputtering target in the shape of a 2″-diameter disc of metallic silver served as a source of metal for evaporation. To create oxide-containing nanoparticles, the sputtering gas (argon) was mixed with oxygen, in a so-called reactive sputtering process. To facilitate the heat exchange with the cryostat He gas was injected from a dedicated inlet. The magnetron-discharge plasma is known to produce reactive oxygen species, such as atomic, ionised, and excited oxygen, which efficiently bind even with noble metals, such as silver and gold [20–22]. In our setup, the metal-oxide molecules created in the magnetron plasma agglomerated into nanoparticles in a cryogenically cold Ar-He mixture blown through the cryostat. The gas flow took the nanoparticles out from the cryostat through a narrow tubular nozzle. Our nanoparticle source was earlier shown to produce particles with the dimensions of ~10 nm [20], as determined by electron-microscopy imaging after the particle deposition.

The present photoelectron spectroscopy study was performed at FlexPES, a soft X-ray undulator-based beamline at the MAX IV Laboratory, the National Swedish synchrotron facility. The nanoparticle source was attached to a port on the beamline experimental station at 90° to the radiation direction. Within ~30 mm downstream from the nozzle, the nanoparticle beam was crossed by the x-rays, which ionized the species in the beam. The photoelectrons were collected by a Scienta R4000 electrostatic electron-energy analyser mounted at 90° to the particle beam, and at the so-called magic angle (≈54.7°) with respect to polarisation of the plane-polarised radiation.

In our previous studies on the particles containing oxides of different metals [20–22,25,23], we observed that the increase of the oxygen fraction in the sputtering gas-mixture usually led to a noticeable decrease of the particle concentration in the beam, so that the O_2 fraction could not be higher than a certain value, specific for each metal. We have attributed it to the so-called target poisoning, a common phenomenon in the sputtering process: the sputtering rate falls due to the oxygen reaction with the metal target itself and due to the re-deposition of oxide molecules onto the target surface. This phenomenon limited the range of possible oxidation conditions in our experiments.

2.2. Valence and Ag 3d-region spectroscopy

In our earlier work [22] at I411 beamline of Maxlab, we performed a detailed PES study on the *valence* response of Ag-oxide nanoparticles created with our setup at similar to the present conditions. Then, hν≈40 eV was chosen for the maximal ionization cross-section of the valence levels. We showed that in the absence of O_2 in the sputtering gas-mixture, a typical valence spectrum of nanoparticles (Fig. 1a) was practically identical in shape to that of the macroscopic polycrystalline silver metal. At hν≈40 eV, the spectrum for the latter and for the metallic nanoparticles consists of an intense Ag 4d band with two maxima and a much weaker and flat 5s band (Fig. 1a). The photon energy of hν≈40 eV, favourable for the latter band [16], facilitated its detection, as well as the detection of the other spectral features. In those experiments, the signal intensity was enough to use relatively high spectral resolution of ≈0.1 eV. In the earlier work [22] and in the current work, the absolute calibration relative to vacuum was made possible by the Ar and He gases co-present in the nanoparticle beam. For the calibration, Ar 3s, Ar 3p, Ar 2p, and He 2s spectral lines were used. On the absolute binding energy scale, the onset of the valence spectrum of the purely *metallic* nanoparticles produced by our apparatus was recorded at

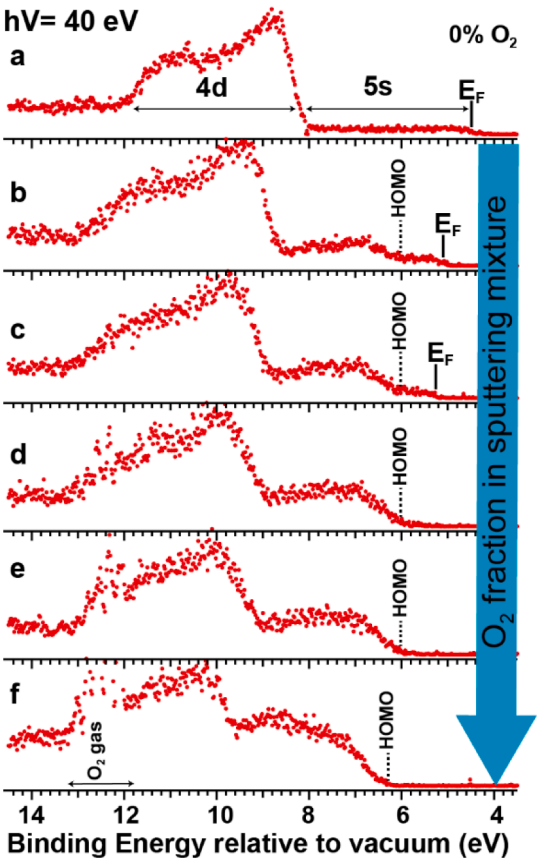

Fig. 1. Adopted from [22]. PES spectra recorded in the valence region at hν= 40 eV and calibrated relative to the vacuum level of free nanoparticles in a beam. The molecular O_2 response is also detected – due to this gas co-presence in the beam.

≈4.5 ± 0.2 eV (Fig. 1a) —denoting the FE/WF value of the particles. When the reactive sputtering was "turned on" (Fig. 1b-f), the spectra of the particles created at higher O_2 fractions closely resembled those of Ag_2O and AgO oxides recorded at hν≤100 eV [2,13]. The characteristic feature for the oxide spectrum is the lower-energy "band" (Fig. 1b-f) detected for the nanoparticles between 6 and 10 eV absolute binding energy. At the strongest oxidation conditions, the onset of this feature is at ≈6.3 ± 0.2 eV. This onset defines the HOMO edge for the oxide (Fig. 1f).

In our earlier studies [21–23] on various metal-oxide particles created with our apparatus, we found that when these particles were formed at lower O_2 fractions they possessed core-shell geometry. In such particles, the core was composed of the oxide, and the shell was metallic, consisting of few monolayers. Such a geometry could be explained by the relative concentrations of the metal-vapour atoms and oxygen close to the magnetron target, as well as by the thermodynamic and kinetic particulars of the production process. In the corresponding valence spectra of metal/metal-oxide particles, this core-shell component distribution manifested itself as a co-presence of the typical oxide and typical metallic responses [20–23]. Amongst others, this was also observed [22] by us for the particles containing silver oxide, where a part of the characteristic flat metallic 5 s band was still seen overlapping with the oxide band. The onset of the metallic band was then detected at 5.2 ± 0.2 eV (Fig. 1b,c). This is ≈0.7 eV higher than ≈4.5 eV of the purely metallic particles (Fig. 1a). With the O_2-fraction increase, the initially low intensity of the 5s response of the shell decreases below our detection limit (Fig. 1d-f). All-in-all, the characteristic behaviour of the valence spectra of the silver-oxide nanoparticles has been consistent with the core-shell structure typically created by our apparatus.

In the present work, carried out at FlexPES beamline of MAX-IV Laboratory, the valence spectra could be recorded at hν=100eV as lowest, which meant significantly smaller ionization cross-sections for both Ag 4d and Ag 5s levels [16]. For the latter level, it led to even further decrease of our ability to detect the metallic-shell signal in the valence spectra. Nevertheless, at the characteristic fabrication conditions – (1) with no O_2 and (2) with the maximal possible O_2 in the sputtering mixture, the spectra recorded in the current work practically reproduced those of our earlier valence study [22].

In the present work investigating the *Ag 3d core-level region*, a range of oxidation conditions similar to our study [22] has been covered (Fig. 2). The O_2 fractions from ~1% up to ~20% were tested. Using hν=420 eV, the Ag 3d spectra of the nanoparticles formed at such conditions were recorded on the absolute binding-energy scale –with the vacuum level at zero (Fig. 2). On that scale, the spectra were calibrated making use of the atomic argon co-present in the nanoparticle beam. For

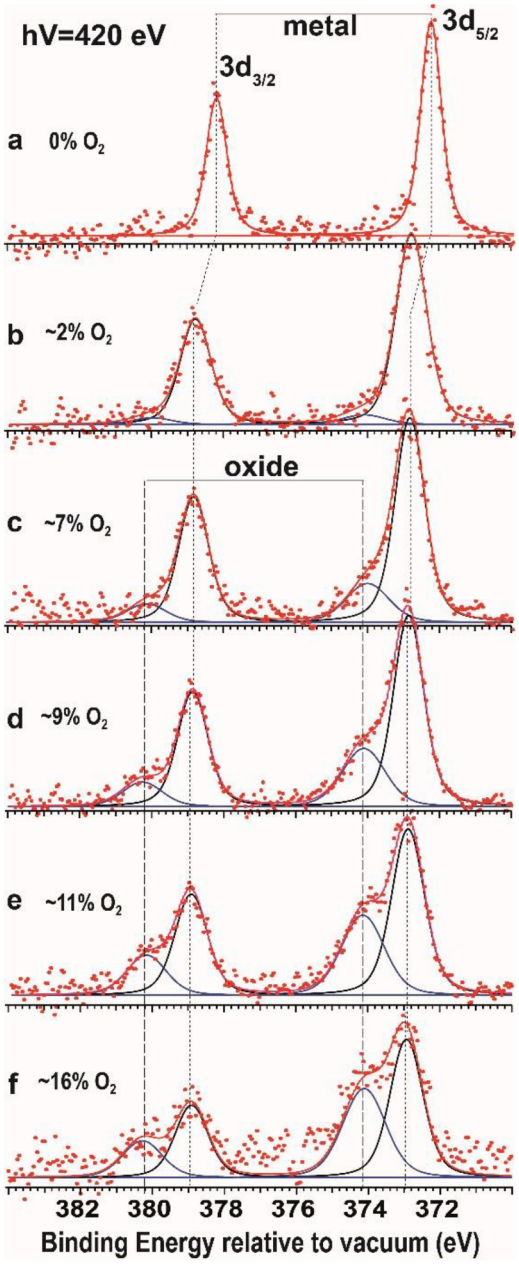

Fig. 2. Ag 3d spectra of free nanoparticles created at different oxidation conditions. The O_2 fraction increases from b to f, and the oxide doublet rises.

that, the Ar 2p spectrum, with the Ar $2p_{3/2}$ line at 248.63 eV [24], was recorded with the same position of the beamline monochromator as for the Ag 3d spectra.

For metallic macroscopic silver, the Ag 3d spectrum is known to be a spin-orbit-split doublet with its two components separated by ≈ 6 eV [1]. This is also how the spectrum of free nanoparticles produced in the absence of O_2 in the sputtering gas appeared in our experiments (Fig. 2a). The Ag $3d_{5/2}$ component of the doublet was detected centred at ≈372.3 eV relative to vacuum (Fig. 2a). As discussed in detail further on in the Results section, this signal could be assigned to metallic-silver response, meaning metallic particles. Upon admixing of O_2 to the sputtering mixture, at few percent O_2, a second, additional doublet with the same separation and intensity ratio of components appeared, roughly at 1 eV higher binding energy than the lower one. With the increasing fraction of O_2 in the sputtering mixture, this second, higher-lying doublet grew in relative intensity (Fig. 2c-e). We have interpreted this second doublet as due to the presence of oxide in the particles. Our conclusion was supported by a similar spectral pattern and its transformation (with the O_2-fraction) observed by us for the other metal-oxide nanoparticles [20–22,25,23]. Already at the smallest O_2 fraction of ~2%, the first, lower-energy doublet, assigned to the metallic silver, shifted up in energy by ≈0.7 eV, and it remained at this spectral position up to the highest oxygen fraction studied.

3. Results and discussion

3.1. Metallic-particle response

In the purely metallic-Ag nanoparticles created by our apparatus, the WF differs by only 0.2–0.3 eV from that of the macroscopic silver (Fig. 1a), which observation, together with the valence-band spectral shape, is evidence for such particles to be just nanoscale pieces of solid metal. Consequently, the conclusions derived from the PES studies of these particles are likely to be valid also for the corresponding *macroscopic* samples. Additionally, the 0.2–0.3 eV WF difference contains information on the particle dimensions and allows estimating them to be ≤10 nm [22].

For the metallic-Ag nanoparticles, in order to compare the absolute Ag 3d binding energy determined in the present work (Fig. 2a) and the energy for the macroscopic silver, given in literature relative to Ag FE-level, the metallic-particle WF/FE has to be subtracted from the vacuum-referenced Ag 3d energy of the particles. As mentioned above, for our metallic particles, the WF_p of 4.5 ± 0.2 eV could be derived from the onset of the valence spectrum (Fig. 1a). The subtraction of 4.5 eV from the metallic-particle Ag $3d_{5/2}$ absolute energy (372.3 eV) gives ≈367.8 eV. This is a satisfactory match to the value found for the macroscopic Ag $3d_{5/2}$ energy referenced to the metal FE in, for example, the widely cited Ref. [2]: 368.0 ± 0.2 eV. There, the spectral broadening due to the non-monochromatized Al K_α radiation work was ≈1 eV.

3.2. Oxide-containing particles, Fermi and HOMO energies

As mentioned above, in our earlier studies [21–23,25], we have established that up to a certain fraction of O_2 in the sputtering mixture, the particles with the oxide core and metallic shell were typically created. (For some metals studied, like Au [21] and Sn [25], sufficiently strong oxidation conditions could be realized so that the metallic shell was not formed anymore.) In these earlier works, the mixed composition (metal and metal-oxide) manifested itself via the co-presence of both the metallic and the oxide signals in the core-level spectra. The levels studied were as a rule doublets, just like in the current case for Ag. For the core-shell geometry, the relative increase of the oxide signal corresponds to the growth of the oxide core and the metallic shell getting thinner.

As described in the Experimental section, in our valence study of Ag-oxides [22], at weaker oxidation conditions (Fig. 1b,c), both the oxide and the metallic signal could be detected, the latter as the characteristic 5s band. With the core-shell geometry, this 5s signal comes from the shell of the particles. The onset value for the 5s-band is then the work-function WF_{sh} of the particle metallic part or its Fermi level. At the same time, it is also the Fermi level for the oxide core –since the core is in contact with the shell. Due to the formation of the core-shell geometry, some change in the metallic-surface WF can be naturally expected. The few monolayers at the surface cannot but be influenced by the underlying substrate, its crystal and electronic structure. In the present case, the increased value of the WF (5.2 ± 0.2 eV) was detected at the weakest oxidation conditions. Additionally, one cannot exclude the change of the WF due to the O_2 possible adsorption on the particles –at the later stage of their motion through the cryostat, when they become significantly colder. A saturated coverage of O_2 on silver (0.5 monolayer) increases the WF by ≈0.25 eV, and a monolayer - by up to 0.5 eV. [26] Earlier, we have observed a WF change for all metal-oxide particles we studied. For their *core-levels*, an upwards shift of the signal from the metallic shell was usually also detected. For example, in gold-oxide nanoparticles, it was as big as ≈1 eV [21]. For silver-oxide, after the initial ≈0.7 eV shift (Fig. 2a,b), the metallic Ag 3d doublet stayed constant in energy, while the oxide doublet grew in relative intensity. Notably, the 5s and 3d responses of the metallic shell shifted up by the *same* 0.7 eV (Figs. 1, 2). This result is in accord with the fundamental understanding of the constancy of the core-level energy relative to the Fermi level. Altogether, the observations also mean that for the core-shell particles we produced, the Fermi-level position remained the same relative to vacuum- for all fabrication conditions.

In the core-level spectra (Fig. 2c-f), the Ag $3d_{5/2}$ oxide feature appears at ≈374.2 eV absolute binding energy – about 1.2 eV higher than the corresponding metallic-shell peak in the spectra. This positive shift of ≈1.2 eV was interpreted by us as the oxide shift – derived directly from one and the same spectrum of the particles, in which the Fermi levels of the metallic-shell and the oxide-core were aligned. If one compares the *absolute* energy of Ag $3d_{5/2}$ oxide-feature (≈374.2 eV, Fig. 2c-f) with that of the corresponding peak of the purely metallic particles (≈372.3 eV, Fig. 2a) then the difference becomes around 2 eV. However, in the oxide-containing particles, the Fermi energy relative to the vacuum is higher by ≈0.7 eV. In order to give an "ultimately correct" shift value one would have to define the "oxide-shift" term more stringently.

The alignment of the Fermi levels of the shell and the core also allows estimating the energy separation of the oxide Fermi level from the HOMO edge. Indeed, for the oxide-containing particles, the HOMO edge relative to vacuum is extracted from the spectrum as the valence-band onset. With this onset at ≈6.3 ± 0.2 eV and the Fermi level at 5.2 ± 0.2 eV, the separation is ≈1 eV. One can recollect here that ≈1 eV between the HOMO and the Fermi level was indeed reported for the plasma-oxidized Ag foil covered with Ag_2O in Ref. [2].

As discussed in the Experimental part, fully oxidized particles could not be produced in the current work. Otherwise, from the valence spectra of such particles it would be possible to deduce the oxide Fermi energy –using the HOMO-FE separation established above. The necessary for such deduction HOMO-vacuum separation would be possible to obtain directly from the spectra.

Due to the swift motion of the free particles across the photon beam, the alignment of the Fermi levels is likely preserved under the x-ray irradiation. Our estimates and observations show that each "sample" –a particle–absorbs only one photon of the beamline radiation in question. This is a crucial difference relative to a common situation in a PES study on supported, immobile oxide samples. In particular, for such *silver-oxide* samples, the continuous charge production under x-ray irradiation leads to the charge accumulation on them [2–4]. As a result, a steady-state positive potential is created on the oxide. Typically, an oxide sample is in contact with another substance, a metal, which is grounded. Such a situation is analogous to a diode, in this case – a Schottky diode. In the absence of potentials on its two constituent parts,

the metal and the oxide Fermi levels are aligned. However, when the diode's semiconductor part is biased, the alignment of the Fermi levels disappears –due to the shift of all the semiconductor levels together. Such a semiconductor/metal contact is realized in the cases discussed in the Introduction. In one typical case, it is an oxide pellet mounted on a metallic sample holder. In the other case, it is a layer of oxide created by the oxygen-plasma on the metallic-silver foil. In these cases, the degree of charging and thus the potential on the semiconductor part differ depending on the interplay of the radiation intensity and conductivity of the oxide sample and its contact to metal. Due to the charging, it is not uncommon to have the apparent binding energy shift of several eV in the spectra.

There is one more difference between the common surface oxides and the metal/metal-oxide particles created in the current work. In the former, the oxide part "faces" the x-ray radiation; in the latter, the metallic shell "sees" it first. It is the surface material, which defines the work function of the layered sample, and it is a metal which is on the surface of the particles. Nevertheless, as mentioned above, the deduced HOMO energy of the oxide and the Fermi energy of the shell, allow calculating the HOMO-FE separation, which is an invariant property. Indeed, this separation is independent of which side is irradiated– the metallic one or the oxide – if the Fermi levels remain aligned. In our work [25] on tin-oxide core-shell particles, we could experimentally test the validity of such invariance. The HOMO-FE separation obtained by us could be compared with that for surface-oxidized tin foil reported in Ref. [27]. In this latter work, the metallic band from the underlying, non-oxidized part of the foil could be detected – overlapping with the spectral response of the surface oxide. The Fermi level of the underlying metal allowed then deducing the HOMO-FE difference, which occurred to be close to ours [25].

Fig. 3 schematically summarizes the observations for the mutual positions of the *core* and *valence* levels (Figs. 1 and 2) which are deduced from our spectroscopic measurements. The figure demonstrates the transformation of the FE, HOMO, and Ag $3d_{5/2}$ energies from the case of metallic particles to that of the core-shell particles. In the left panel, the Figure shows the levels for the purely-metallic particles, the spectra of which are presented in Figs. 1a and 2a. Then the $WF_p \approx 4.5$ eV and the Ag $3d_{5/2}$ energy is ≈372.3 eV relative to vacuum. In the middle panel, the energies are given deduced for the metallic shell in the oxide-core/metal-shell particles. The WF_{sh} and the corresponding Ag $3d_{5/2}$ level of the shell are shifted up in energy by the same 0.7 eV –relative to the purely-metallic case. In the right panel, the detected from the experiment HOMO and Ag $3d_{5/2}$ energy for the oxide core of the same core-shell particles as in the middle panel are presented. The energy scheme is put together in the assumption of the Fermi energies alignment for the shell (middle panel) and the core (right panel).

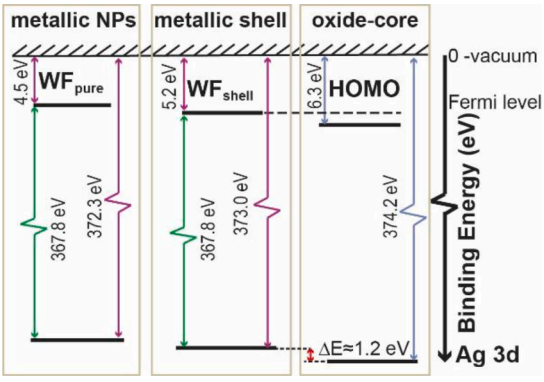

Fig. 3. Schematic presentation of the energy-level structure for the metallic nanoparticles (left), and for the core-shell particles with a metallic-silver shell and silver-oxide core (centre and right). The Fermi levels for the core and shell are aligned.

3.3. Ag_2O or AgO?

As discussed in the Introduction, the spectroscopic response of the two silver oxides Ag_2O and AgO in the Ag 3d region was widely accepted to differ only slightly, with the oxide shifts being negative in both cases. Structurally, the stronger AgO-oxide is considered having two silver-oxygen coordinations (a mixed-valence compound): one analogous to Ag(I)-oxide and the other –to Ag(III)-oxide, so on the average there are two atoms of oxygen per two silver atoms: Ag_2O_2 or AgO [8]. In view of our Ag 3d results deviating from all known to us previous works on Ag-oxides, the assignment of the chemical composition for our nanoparticles is not trivial. The narrow Gaussian spectral profile of the oxide "lines" speaks for only one coordination/chemical state in the particles, likely for Ag(I)-oxide since the shift is relatively small –about 1 eV. The co-presence of two different states can be expected to broaden the total oxide response, as assumed in [12]. Such broadening was observed by us for free nanoparticles containing SnO and SnO_2 oxides [25]. At the same time, in our studies on gold-oxide nanoparticles [21], the formation of the Au(III)-oxide already at relatively low O_2 concentrations was demonstrated – using the Au 4f core-level spectra. In the current work, the signal-to-noise ratio in the Ag 3d spectra for higher oxygen fractions does not exclude the presence of additional spectral features 1÷2 eV higher up in binding energy relative to the oxide doublet. The observed extra intensity could be due to the Ag(III) presence in the particles. It has been underlined [2,8] that the opened 4d-shell in the Ag(III)-oxide should lead to appearance of the satellite lines in the Ag 3d spectra of such an oxide - due to the possible *initial* states with either $4d^8$ or $4d^9$ –electronic configurations. In work [8], such satellites were reported to have been observed, while the overall assignment there followed the consensus of small negative shifts. However, in the studies on the pressed AgO powders [1,4] or AgO produced by other methods [12,14] no satellites of that type were reported. The satellites' intensity can be expected to be considerably lower than that of the main lines. This was experimentally confirmed in, for example, the PES investigation of Pd (II)-oxide [28], in which oxide the metal ion has the same amount of electrons in the 4d shell as the Ag ion in the Ag(III)-oxide. The Pd (II)-oxide case is unambiguous since there is no uncertainty with the assignment for it: positive oxide shifts are observed. The relative satellite intensity for Pd-oxide is low, so, if it is similar for Ag 3d, it would be hardly possible to detect the satellite peaks in our study. Moreover, the satellites in Pd-oxide were observed ≈9 eV above the corresponding main peaks. This is outside the spectral region of not only of the current work, but also of the work [8], in which the observation of Ag (III)-satellites was claimed. All-in-all, the satellite arguments applied to our case do not lead to a conclusive assignment of the particle composition.

Another way to find out what oxide is created can be based on the energy difference between the HOMO and the Fermi levels. The HOMO-FE separation of ≈1 eV, deduced in the current work, means that the energy gap between the HOMO and LUMO bands is higher than that. The multiple measurements of the gap in different silver oxides produced by various methods gave values from 1.3 eV [29] up to 3.3 eV [30]. The latter work, where the silver-vapour atoms were oxidized in oxygen plasma, reported a fabrication of a thin film containing co-existing Ag_2O and AgO oxides. In general, silver oxides have been a subject of investigation aimed at finding an optically transparent conducting oxide, what means, with a gap above 2 eV. There are works assigning a gap lower than, or just above 2 eV to Ag_2O and transparency in UV for AgO [31–33]. The conclusion possible to make from the literature on the gaps is that there is no clear consensus on the issue, and the current-work value of the FE is compatible with both oxides. At the same time, the PES arguments discussed above favour the conclusion of only one, weaker oxide dominating the composition.

4. Conclusions

The outcome and conclusions of the current work are the result of experiments on a beam of free nanoparticles created *in-situ* by a sputtering-based vapour aggregation method and studied using synchrotron-based X-ray PES. Such experiments provide a chemically clean and continuously and swiftly renewed sample, thus allowing avoiding fabrication-related contaminations and charge accumulation on the sample under the ionizing irradiation. The access to the *absolute* binding energies of the oxide and its parent metal, their Fermi edges, and the oxide HOMO energy in the PES measurements on a nanoparticle beam, allowed controlling the fine interconnected changes of all these levels, the changes which are otherwise difficult to separate.

Using these experimental advantages, the oxide shift, i.e. the electron binding energy difference between the metallic-silver and silver-oxide responses in the Ag 3d region, has been studied. For that, free nanoparticles containing both the metallic and the oxide parts were fabricated and probed. At the experimental conditions, which allowed keeping the Fermi levels aligned, the oxide shift has been determined to be positive and equal to ≈1.2 eV. This is in contrast to the previous experimental works reporting negative shifts below 1 eV in magnitude. Both the positive sign and the value of the oxide shift extracted in the current work are typical for most metal-oxides, including other noble metals. The symmetric and relatively narrow shape of the oxide Ag 3d response in the current work indicates the presence of only one chemical state in the particles, likely Ag(I)-oxide. The discrepancy with the previous works can be possibly explained by the composition and calibration uncertainties characteristic for a larger part of the works, many of which were performed on *ex-situ* samples, used the radiation sources of ≈1.4/1.2 keV, and had noticeably lower resolution than the present work.

Author contributions

The manuscript was written through contributions of all authors. All authors have given approval to the final version of the manuscript. All authors contributed equally.

Declaration of Competing Interest

There is no conflict of interest for the manuscript.

Data availability

Data will be made available on request.

References

[1] G. Schön, Acta Chem Scand 27 (1973) 2623.
[2] L.H. Tjeng, M.B.J. Meinders, J. van Elp, J. Ghijsen, G.A. Sawatzky, Phys Rev B 41 (1990) 3190.
[3] G.B. Hoflund, J.F. Weaver, W.S. Epling, Surf Sci Spectr 3 (1994) 163.
[4] G.B. Hoflund, J.F. Weaver, W.S. Epling, Surf Sci Spectr 3 (1994) 157.
[5] B. Hodnett, Heterogeneous Catalytic Oxidation, John Wiley and Sons Ltd, Chichester, U.K., 2000.
[6] G.B. Hoflund, Z.F. Hazos, G.N. Salaita, Phys Rev B 62 (2000) 126, 11.
[7] Jill Chastain, Handbook of XPS, Perkin-Elmer Corporation, 1992. Ed. by.
[8] T.C. Kaspar, T. Droubay, S.A. Chambers, P.S. Bagus, J Phys Chem C 114 (2010) 21562.
[9] M. Schmid, A. Reicho, A. Stierle, I. Costina, J. Klikovits, P. Kostelnik, O. Dubay, G. Kresse, J. Gustafson, E. Lundgren, J.N. Andersen, H. Dosch, P. Varga, Phys Rev Lett 96 (2006), 146102.
[10] H. Grönbeck, S. Klacar, N.M. Martin, A. Hellman, E. Lundgren, J.N. Andersen, Phys Rev B 85 (2012), 115445.
[11] D. Lützenkirchen-Hecht, Surf Sci Spectr 18 (2011) 96.
[12] D. Lützenkirchen-Hecht, Surf Sci Spectr 18 (2011) 102.
[13] L.S. Kibis, V.I. Avdeev, S.V. Koscheev, A.I. Boronin, Surf Sci 604 (2010) 1185.
[14] M. Bielmann, P. Schwaller, P. Ruffieux, O. Gröning, L. Schlapbach, P. Gröning, Phys Rev B 65 (2002), 235431.
[15] P.H. Citrin, G.K. Wertheim, Y. Baer, Phys Rev B 27 (1983) 3160.
[16] J.J. Yeh, I. Lindau, Atom Nucl Data Tables 32 (l) (1985).
[17] N.W. Ashcroft, N.D. Mermin, Solid State Physics, Harcourt, Orlando, FL, 1976.
[18] M.A. Stranick, A. Moskwa, Surf Sci Spec 2 (1993) 45.
[19] M.A. Stranick, A. Moskwa, Surf Sci Spec 2 (1993) 50.
[20] M. Tchaplyguine, M.-.H. Mikkelä, O. Björneholm, Multicomponent nanoparticles for novel technologies, in: K. Sattler (Ed.), 21st Century Nanoscience – A Handbook, Taylor & Francis, 2020.
[21] M. Tchaplyguine, M.-.H. Mikkelä, Ch. Zhang, T. Andersson, O. Björneholm, J Phys Chem C 119 (2015) 8937.
[22] M. Tchaplyguine, C. Zhang, T. Andersson, O. Björneholm, Chem Phys Lett 600 (2014) 96.
[23] Ch. Zhang, T. Andersson, S. Svensson, O. Björneholm, M. Tchaplyguine, Phys Rev B 87 (2013), 035402.
[24] L. Avaldi, G. Dawber, R. Camilloni, G. King, M. Roper, M. Siggel, G. Stefani, M. Zitnik, J Phys B 27 (1994) 3953.
[25] Ch. Wright, Ch. Zhang, M.-.H. Mikkelä, E. Mårsell, A. Mikkelsen, S. Sorensen, O. Björneholm, M. Tchaplyguine, J Phys Chem C 121 (2017) 19414.
[26] B. Xinhe, D. Shuzhong, D. Jingfa, Surf Sci 199 (1988) 493.
[27] P. De Padova, M. Fanfoni, R. Larciprete, M. Mangiantini, S. Priori, P. Perfetti, Surf Sci 313 (1994) 379.
[28] Takayuki Uozumi, Tetsuo Okane, Kenji Yoshii, Teikichi A. Sasaki, Akio Kotani, J Phys Soc Jpn 69 (2000) 1226.
[29] E. Fortin, F.L. Weichman, Physica Status Solidi A 5 (1964) 515.
[30] S.B. Rivers, G. Bernhardt, M.W. Wright, D.J. Frankel, M.M. Steeves, R.J. Lad, Thin Solid Films 515 (2007) 8684.
[31] A.J. Varkey, A.F. Fort, Sol Energy Mater Sol Cells 29 (1993) 253.
[32] Gao Xiao-Yonga, Feng Hong-Lianga, Ma Jiao-Mina, Zhang Zeng-Yuana, Lu Jing-Xiaoa, Chen Yong-Shenga, Yang Shi-Ea, Gu Jin-Hua, Physica B 405 (2010) 1922.
[33] R.K. Jamala, F.A-H. Mutlaka, F. T.Ibrahima, U.M. Nayef, Int J Light Electr Opt 218 (2020), 164971.